Graphene-Montmorillonite Composite Sponge for Safe and Effective Hemostasis

Guofeng Li,[†] Kecheng Quan,[†] Yuping Liang,[†] Tianyi Li,[†] Qipeng Yuan,[†] Lei Tao,[‡] Qian Xie,[§] and Xing Wang*,[†] [ID]

[†]Beijing Laboratory of Biomedical Materials, Beijing University of Chemical Technology, Beijing 100029, People's Republic of China

[‡]The Key Laboratory of Bioorganic Phosphorus Chemistry & Chemical Biology (Ministry of Education), Department of Chemistry, Tsinghua University, Beijing 100084, People's Republic of China

[§]Nephrology Department, Peking University Third Hospital, Beijing 100191, People's Republic of China

ABSTRACT: Montmorillonite (MMT) is considered to be the most effective hemostat among natural phyllosilicates. However, there is a barrier against using MMT for the commercial hemostatics because the invaded MMT powders might cause thrombosis in vessel. Until now, it is still a challenge to manage the release of MMT and eliminate its side effect. Herein, we present a graphene-MMT composite sponge (GMCS), synthesized under a hydrothermal reaction, fixing MMT powders into the cross-linked graphene sheets. We demonstrate that only a few embedded MMT can evoke remarkable platelet stimulation at the sponge interface, while maintaining fast plasma absorbency of the innate sponge. In the synergy of the above hemostatic mechanisms, the GMCS can rapidly stop bleeding in approximately 85 s in rabbit artery injury test. More importantly, computed tomography angiography certifies that the GMCS does not cause thrombus or blood clot in vessels. Cytotoxicity assay further highlights its biocompatibility. In-depth analysis proposes that two-dimensional graphene overmatches one-dimensional linear polymers in the composite construction, and dimension transformation of blood distribution plays a crucial role for reinforcing the hemostatic performance. This GMCS hemostat not only opens a new perspective for graphene composite, but also makes a new chance of using clays for trauma therapy.

KEYWORDS: graphene, montmorillonite, composite, hemostatic sponge, hemostasis

1. INTRODUCTION

Excessive bleeding usually increases the risk of suffering hemorrhagic shock coagulopathy, infection, and multiple organ failures.[1−3] As reported, hemorrhage results in 30−40% of deaths and is the leading cause of trauma-associated death.[4,5] Thus, applying hemostatic agents is important for rapid and effective control of hemorrhage. Currently, the common used hemostatic agents include inorganic clay, also known as two-dimensional (2D) nanosilicates such as kaolinite, sepiolite, and smectite (laponite, montmorillonite (MMT), saponite, and hectorite);[6,7] organic materials such as chitosan, fibrinogen, and gelatin; and their composite.[7,8] Previous studies reported that smectite is the most effective hemostatic agent due to its swell property and charged stimulation of activating blood coagulation.[9−11] It can result in 100% stable hemostasis when compared to other phyllosilicates,[12−14] and even commonly used biopolymer chitosan in some cases.[15] However, because the free smectite might result in cytotoxicity and even thrombosis in vivo,[14,16] the Food and Drug Administration (FDA) has limited its commercial hemostatic products since 2007. Nevertheless, smectite is still very useful and necessary for developing biomedical materials.[6] For example, as one kind of semctites, MMT is widely used in the fields of skin protection and cleansing, antibacterial, and wound healing.[17−20] In those cases, MMT is safely used by preventing it from being in touch with cells directly.[16] We thus hypothesize that a suitable supporter may anchor MMT to avoid its side-effects, reviving MMT as the most effective and safe hemostasis.

Recently, we developed a new hemostatic agent based on the cross-linked graphene sponge (CGS).[21] It is considered to be a promising supporter due to its porous structure. Only by physical absorption of plasma can it rapidly stop bleeding in approximately 2−4 min in rat-tail cutting model. If new stimulation is introduced into the CGS, its hemostatic performance can be further enhanced.[22] Therefore, fixing MMT into stacking graphene sheets of the CGS should be safe and effective for a reinforced hemostasis, especially through combining outer fast plasma absorption and inner intensive stimulation.

Herein, we report a graphene-MMT composite sponge (GMCS), which is synthesized by employing graphene oxide (GO) sheets, ethylenediamine (EDA) linkers, and MMT powders under a typical hydrothermal reaction, thus fixing MMT powders into the layered graphene (Scheme 1). In

Scheme 1. Schematic Representation of the Preparation Route and the Microstructure of the GMCS[a]
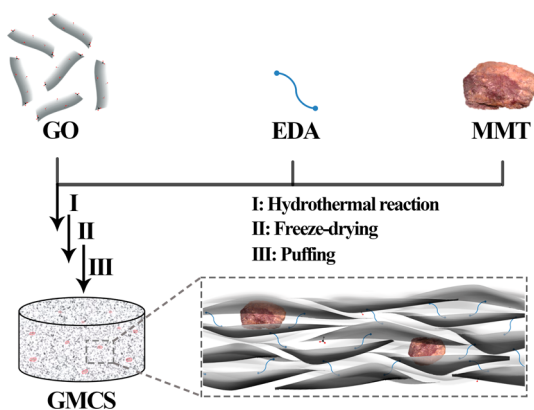
[a]The GMCS is first synthesized by hydrothermal reaction employing GO sheets, EDA linkers, and MMT powders. After freeze-drying and puffing treatments, the final product then is obtained. The enlarged microstructure image shows MMT is fixed into the layered graphene.

comparison with the previously reported hemostatic graphene sponge, this GMCS inherits the fast plasma absorbability due to its porous graphene structure. The advance is its embedded MMT as new active sites, which is more powerful to trigger blood coagulation. More importantly, the superexcellent match between graphene sheet and MMT sheet makes this graphene-MMT composite renew an avenue for the safe use of MMT in the field of trauma hemostasis and therapy.

2. EXPERIMENTS

2.1. Materials. Graphite powder (80 mesh) was purchased from Qingdao Jinrilai Co., Ltd., Shandong, China. Sulfuric acid (H_2SO_4, 98%), potassium permanganate ($KMnO_4$, 99.9%), sodium nitrate ($NaNO_3$, AR), hydrochloric acid (HCl, 37%), and hydrogen peroxide (H_2O_2, 30%) were purchased from Sigma-Aldrich Co. The GO solution was prepared with a modified Hummers' method,[23] and the concentration of the GO solution was 7.5 mg mL^{-1}. The MMT powder was obtained from a commercial pharmaceutical named Biqi (Simcere Co., Ltd., Jiangsu, China). It was extracted and washed with ethyl alcohol in a Soxhlet extractor for 48 h. The obtained powder then was dried at 95 °C for 48 h. Other common reagents were purchased from Sinopharm Chemical Reagent Co., Ltd., and were used as received.

2.2. Preparation and Characterization of the GMCS. Briefly, about 60 mg of MMT was added into 60 mL of GO solution and mixed by a high-speed blender at 16 000 rpm for 10 min. After adding

900 μL of EDA, the mixture was mixed for another 10 min and sealed in a hydrothermal synthesis reaction kettle and heated at 96 °C for 6 h to obtain a hydrogel. The hydrogel then was freeze-dried for 48 h and followed by an alcohol washing for 48 h. The GMCS (4 cm diameter, 2 cm thickness) was obtained under 800 W microwave puffing for 5 s. Finally, the obtained GMCS was washed again with alcohol to remove the exposed MMT. Through changing the addition amount of MMT powders from 1 mg·mL^{-1} to 2, 5, and 10 mg·mL^{-1} in GO solution, the GMCS-2, GMCS-5, and GMCS-10 were prepared, respectively, with the above-mentioned method.

Scanning electron microscopy (SEM, Hitachi S-4700) and transmission electron microscopy (TEM, FEI TECNAI G2) were used to observe the interior structure of the GMCS. Energy-dispersive spectrometry (EDS, Hitachi S-4700) was used to analyze the surface element content between the GMCS and MMT. The acceleration voltage of the EDS mapping images (Figure 1D−H) was 20.0 kV. The acceleration voltage of the other SEM images was 10.0 kV. The acceleration voltage of TEM image was 200 kV. Thermogravimetric analysis (TGA, Mettler Toledo TGA/DSC1/1100SF) was used to analyze the MMT content of the GMCS. Zeta potential (Malvern NanoSizer ZS2000) was used to detect the negative potential of the GMCS, the CGS, and MMT.

The liquid absorbability of the GMCS was evaluated by measuring the absorption ability and the absorption rate. The absorption ability was measured by calculating the weight difference between the initial weight of the GMCS and the weight after adequately absorbing the liquid. The absorption rate was recorded by a high-speed camera (40 ms per frame) to observe the whole absorption process of a liquid droplet.[21]

2.3. Evaluation of the Hemostatic Performance. First, the hemostatic performance was evaluated by the rabbit femoral artery injury model. Five New Zealand rabbits weighing 2.0−2.5 kg were purchased from the Beijing Fuhao Experimental Animal Breeding Center (Beijing, China) and were treated and cared for in accordance with the National Research Council's Guide for the care and use of laboratory animals. All rabbits were anesthetized with 10% chloral hydrate (intraperitoneal injection with 0.5 mL per 100 g) before surgery. Approximately 5 cm of the femoral artery was dissected free from surrounding tissues, and the femoral artery was partially transected (50% of its circumference) to create the injury and hemorrhage. At the beginning of 30 s, pretreatment blood loss was measured (with no surgical manipulation) to make sure all rabbits were in the same condition. A piece of the GMCS (4 cm diameter, 2 cm thickness) then was slightly compressed on the wound. The GMCS was slightly uplifted every 10 s to observe the injury condition. When the wound stopped bleeding, the hemostatic time and weight of the blood loss were recorded. After that, 0.5 L of physiological saline was used to clean the wound carefully, and the wound was closed in layers by suturing. Computer tomography (CT) angiography was performed on the rabbits that survived the 2 h observation period. After 1 month, all rabbits survived, and the wound recovery was observed.

Second, the hemostatic performance was evaluated by in vitro dynamic whole-blood clotting model. A 50 μL volume of rabbit's arterial blood was directly dropped on the GMCS or on a beaker as the control group. After the blood was interacted with the materials for a period of time (30, 60, 120, 180, and 240 s), 10 mL of distilled water was added slowly without disturbing the clotted blood. Each sample was shaken slightly to dissolve the free red blood cells (RBCs). The hemoglobin absorbance of each samples was measured by an ultraviolet spectrophotometer at 542 nm. As a reference value, the absorbance of 50 μL of fresh blood in 10 mL of distilled water was measured. The content of hemoglobin was quantified by the following equation: hemoglobin absorbance = $I_s/I_r \times 100\%$, where I_s is the absorbance of the samples, and I_r is the absorbance of the reference value. This experiment was repeated three times under the same conditions.[21]

2.4. Hemolysis Assay in Vitro. Fresh anticoagulated blood from SD rats (5 mL) was added to 10 mL of phosphate buffered saline (PBS, pH 7.4) and centrifuged at 500g for 10 min to collect RBCs
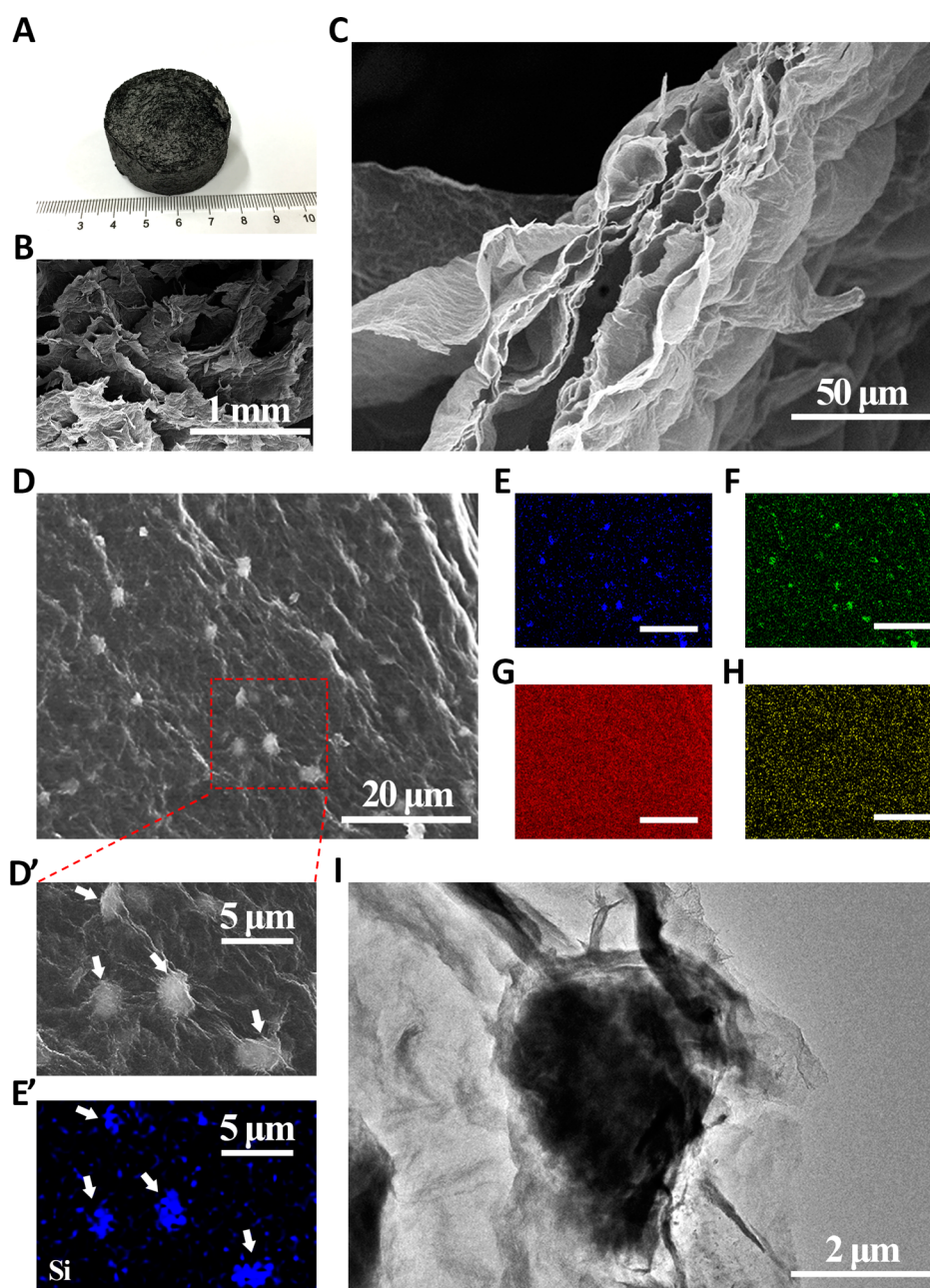
Figure 1. (A) Photograph of the GMCS (4 cm diameter, 2 cm thickness). (B) SEM image of the interior porous structure. (C) The cross-sectional SEM image of the GMCS cell wall. (D) SEM image of the cell wall surface. (D′) The enlarged SEM of image D. Some embedded MMT powders are marked with white arrows. (E−H) EDS mapping of Si, O, C, and N elements of image D. The scale bar is 20 μm. (E′) The enlarged image of E. It is corresponding to image D′. (I) TEM image of the graphene-covered MMT powder.

from serum. This purification step was repeated three times, and then the obtained RBCs were diluted to 50 mL in PBS. To test the hemolytic activity of the GMCS, the CGS, and MMT, 0.2 mL of diluted RBCs was added into 0.8 mL of the sample's suspension solutions in PBS at different concentrations (ranging from 15.6 to 1000 μg mL^{-1}). The sample's suspension solutions were prepared by adding the sample powders (pulverized by agate mortar) in PBS and sonicating for 2 h. Deionized water (+RBCs) and PBS (+RBCs) were used as the positive and negative controls, respectively. All of the samples were incubated on a rocking shaker at 37 °C for 3 h. After incubation, the samples were centrifuged at 10 000g for 5 min. The hemoglobin absorbance was measured at 540 nm with a UV−vis spectrophotometer (UV-2450, Shimadzu). Percent hemolysis was calculated according to the following formula: hemolysis (%) =

(sample abs$_{540\ nm}$ − negative control abs$_{540\ nm}$)/(positive control abs$_{540\ nm}$ − negative control abs$_{540\ nm}$) × 100%.[24]

For the hemoglobin absorption test, the material powders (1000 μg mL^{-1}) were added to the hemoglobin solution, which was set apart from the above-mentioned 1000 μg mL^{-1} MMT group. After the samples were incubated on a rocking shaker at 37 °C for 3 h, the hemoglobin absorbance was determined by the same method.

2.5. Cytotoxicity Assay. L929 mouse fibroblast cells (purchased from Cell Resource Center, IBMS, CAMS/PUMC, Beijing, China) were adjusted to 5 × 10^5 cells mL^{-1} in complete medium (CM), which consisted of 90% RPMI-1640 medium, 10% fetal bovine serum (FBS), and 1% antibiotics (100 units mL^{-1} penicillin and 100 units mL^{-1} streptomycin). The cell suspension was added into 24-well plates (1 mL per well) and incubated for 12 h at 37 °C in an air environment of 5% CO$_2$. Next, 1 mL of the GMCS or the MMT suspension in CM
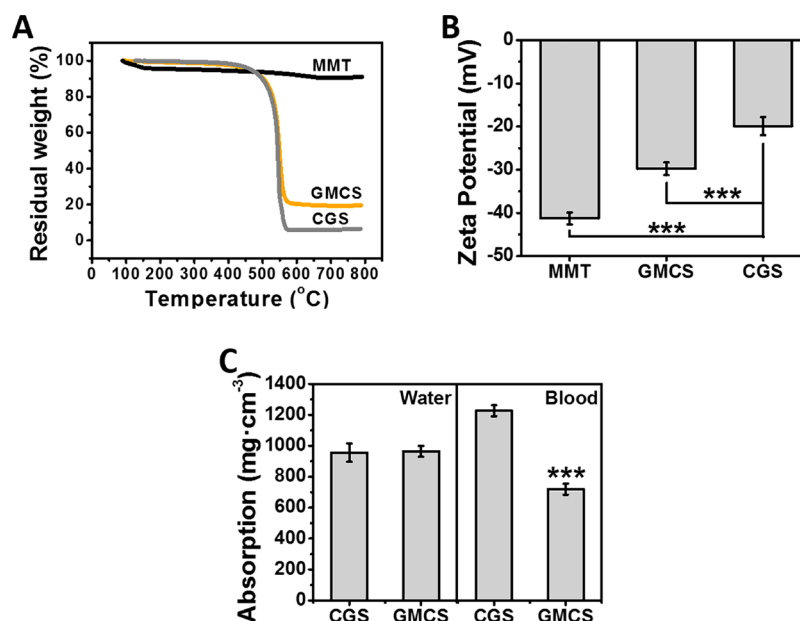
Figure 2. (A) TGA curves and (B) zeta potential of the GMCS, the CGS, and MMT. (C) The water/blood absorption amounts of the GMCS and the CGS. Data values ($n = 3$) corresponded to mean ± SD. Two-way ANOVA; ***$P < 0.001$.

(prepared as mentioned above, section 2.4) was added into the plates to replace the original CM. The concentrations of 250 and 62.5 $\mu g\cdot mL^{-1}$ were used here. After 24 h of incubation, the cells were slowly washed twice with PBS and observed by an electron microscope.

2.6. Interfacial Interaction between Blood Cells and the GMCS. For the blood cells' selected adhesion test, a small piece of the GMCS (1×1 cm², 0.25 cm thickness) was immersed in 10 mL of PBS for 2 h at 37 °C. Next, about 0.5 mL of ACD-whole blood or PRP (1×10^5 platelets μL^{-1}) was added and incubated with the materials for another 1 h at 37 °C. The samples were then rinsed three times with PBS and immobilized with 2.5% glutaraldehyde for 2 h at 4 °C. After that, the samples were then dehydrated with 50%, 60%, 70%, 80%, 90%, and 100% ethanol for 10 min and were freeze-dried for 12 h prior to SEM observation.[25]

For the blood cells' morphology observation, a droplet of ACD-whole blood or PRP was directly dropped on the GMCS (4 cm diameter, 2 cm thickness) surface. After being incubated for 3 min at 37 °C, the samples were treated according to the above-mentioned method prior to SEM observation.

3. RESULTS

3.1. Material Characterization. Figure 1A shows the typical GMCS sample. Although MMT powders were employed, this graphene sponge perfectly inherited the architectural features of hierarchical porous structure of the CGS. Figure 1B exhibits the interior porous structure of the GMCS, giving distinct ripple-like cell walls. In the cross-section of the cell wall (Figure 1C), there are abundant small cavities with sizes in the range of tens to hundreds of micrometers. Figure 1D shows the image of the cell wall surface, where the MMT powders ranging from 2 to 3 μm were distributed in the GMCS. EDS mapping of Si elements (Figure 1E), one of the eigenelements of MMT,[26,27] further confirmed the location of MMT. Moreover, according to the EDS mapping of the cell wall surface (Figure 1E−H), we can see that MMT powders distributed uniformly in the GMCS. In the enlarged image of the cell wall surface (Figure 1D′ and E′), MMT was found embedded in graphene sheets (white arrows). There were evident graphene wrinkles surrounding MMT powders. The

TEM image (Figure 1I) further proved that the MMT powder was covered and anchored to the graphene sheets.

The physicochemical properties of the GMCS were investigated. In the TGA test (Figure 2A), MMT only had a slight weight loss until 800 °C,[28] while the CGS decomposed after 500 °C. Thus, it could be calculated that the GMCS sample contained about 13.5% (w/w) MMT from the difference in weight loss. Because MMT has the negative surface charge,[14] the used MMT powders yielded an electric negative potential of −41.3 ± 1.3 mV. After a composite was made with the CGS, the integrated zeta potential of the GMCS decreased to −29.8 ± 1.5 mV (Figure 2B). Yet as compared to the original CGS (−19.9 ± 2.1 mV), the 13.5% MMT intensively strengthened the negative charge density of the final GMCS. Therefore, we deduced that this composite sponge, to a large extent, would accelerate blood coagulation.

The hierarchical porous structures endow the GMCS with outstanding absorption capability. The water absorption amount of the GMCS (964.4 ± 35.8 mg cm^{-3}) is comparable to that of the CGS (955.4 ± 59.0 mg cm^{-3}, Figure 2C), suggesting that adding MMT did not affect the water absorption amount of the GMCS. However, for the blood absorption tests, it was quite obvious that a 41.3% decrease happened to the GMCS (719.5 ± 35.4 mg cm^{-3}) when compared to that of the CGS (1226.7 ± 35.4 mg cm^{-3}). This case is due to that MMT promotes blood clotting in the GMCS and the clot plugs the inner space of the GMCS. This phenomenon indicated that the GMCS should be in favor of hemostasis. Besides that, the absorption rate tests showed that the GMCS could rapidly absorb either a droplet of water or blood within 40 ms, same as that of the CGS.[21]

3.2. Hemostatic Performance. The in vivo evaluations of hemostatic performance include laceration (liver or skin) model, vascular (artery or vein) injury model, and so on.[12−15,29] Normally, rats are often used as a primary model, followed by bigger animals as the upgraded model. In our previous studies, the rat-tail cutting model was used to evaluate the hemostatic performance of the graphene-based sponge.[21,22] Considering
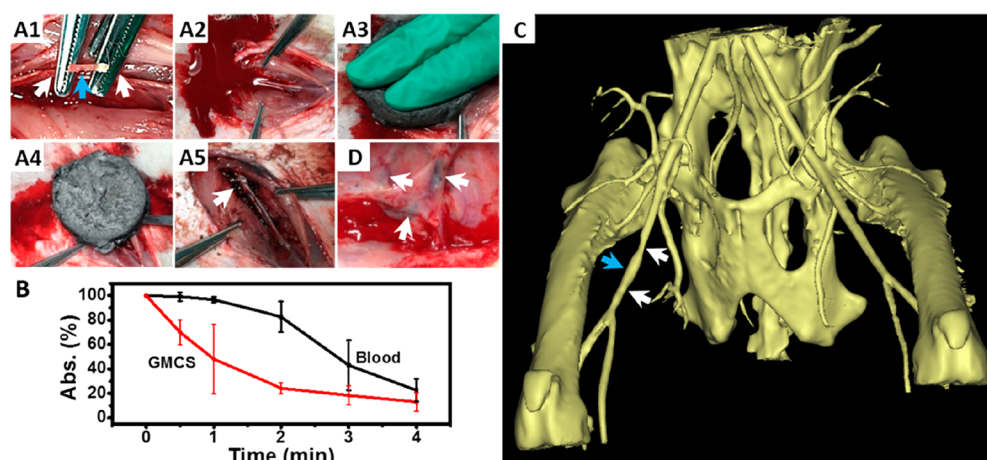
Figure 3. (A) Hemostatic experiment in rabbit artery injury model. (A1) Separated femoral artery and transected artery. (A2) The wound caused hemorrhage. (A3) The GMCS was compressed on the wound. (A4) Hemostasis was achieved. (A5) The wound was cleaned, and a clot formed (white arrow). (B) In vitro dynamic whole-blood clotting evaluation of the GMCS and control. (C) CT image of blood flow through the femoral artery 2 h after treatment. Blue arrow shows the injury site. Two white arrows denote the deformed artery caused by the forceps. (D) Image of the wound after one-month recovery. The white arrows denote the residue GMCS.

that the GMCS has good absorbency and high density of negative charge, 2.0−2.5 kg New Zealand rabbits ($n = 5$) were employed in this experiment. Hemostatic performance of the GMCS was thus evaluated in an in vivo rabbit artery injury model (Figure 3). Typically, the rabbit's femoral artery was first separated from surrounding tissues and partially transected (Figure 3A1, ∼50% of vessel circumference, marked with the blue arrow) to cause hemorrhage (Figure 3A2). Within the initial 30 s, no treatment was carried out to ensure normal blood loss, which was up to 10.6 ± 1.2 mL (if in the standard gauze control group, this kind of injury was bleeding continuously and resulted in 100% mortality; also see ref 30). Next, the GMCS was compressed on the wound (Figure 3A3) to make sure the GMCS fully contacts with the bleeding site. Although different from the hydrogel system that possesses fluid characteristic and can undergo fast gelation in situ,[29,31] the GMCS sponge, to a certain degree, can also transform under very small pressure when handling complex wounds. In this experiment, the transformation of the GMCS was no more than 20% with the operated pressure. The blood was absorbed rapidly by the GMCS. After approximately 85 ± 9 s, the wound stopped bleeding (Figure 3A4), and a clot formed on the interface (Figure 3A5), suggesting a completed hemostasis. For this operation, one piece of the GMCS (4 cm diameter with 2 cm thickness) could perform a better bleeding control within 1.5 min, and the total blood loss was 12.1 ± 2.9 g. The in vitro dynamic whole-blood clotting test also confirmed that the GMCS can effectively promote blood clotting. As show in Figure 3B, when fresh rabbit's arterial blood dropped on the GMCS, the hemoglobin absorbance value decreased sharply within the initial 2 min, suggesting a fast coagulation of the blood in the GMCS, whereas the blood control group required more than 4 min. These results demonstrated that the GMCS is an effective hemostatic material.

As MMT was used in this composite, the thromboembolic risk of the GMCS should be concerned. On the basis of an approved detecting technique, computer tomography (CT) angiography was performed to detect the blood flow of the cured rabbit. Figure 3C shows a typical result of the rabbit's blood vessels after the GMCS treatment. All of the blood vessels were clear when contrast agents flowed through them.

There was no disconnecting part in the angiographic image, meaning no blocking in blood vessels. Moreover, no angiostenosis was found there, except two points near the injury site (blue arrow) caused by the two forceps (white arrows in Figure 3C corresponding to those in Figure 3A1). These phenomena demonstrated that no thrombus or blood clot was formed in the vessels, especially near the injured artery. After 1 week, the operative legs recovered normal motor function, and the mortality rate of the rabbits was 0%. In addition, the residual GMCS, although nondegradable and unabsorbable in vivo, did not cause inflammation of the surrounding tissue (Figure 3D). This fact exhibited a good biocompatibility of the GMCS, indicating the fixed MMT was stable in the graphene sheets and did not cause thrombus in vivo. Therefore, we consider that this composite is a new way for MMT to be used for hemostasis, and the GMCS can be used as a superb agent for trauma therapy.

3.3. In Vitro Hemolysis Assay. Hemolysis assay in vitro is a universal method to assess the hemocompatibility of materials.[32] Direct exposure of the free MMT powders to the RBCs solution resulted in dose-dependent developing of hemoglobin (Figure 4). An about 250 μg mL^{-1} dose of MMT caused 96.7 ± 5.0% hemolysis. This result confirmed that the free MMT is biotoxic and may cause thrombosis.[14] In contrast, the RBCs treated with the same dose of the GMCS did not show hemolysis. When the dosage of the GMCS was up to 1000 μg mL^{-1}, only 3.0 ± 2.3% hemolysis was found. To rule out the possibility of protein absorption onto the GMCS, we further put the GMCS powders (1000 μg mL^{-1}) into the hemoglobin solution. After the solution was incubated for 3 h, the hemolytic ratio only changed by −1.8 ± 3.8% ($n = 3$). Therefore, even if this fact was taken into account, the hemolytic ratio of the GMCS was still far lower than that of the MMT powders because of the out-layered CGS shell.[21,33,34]

3.4. Cytotoxicity Evaluation. In addition, L929 cells were employed to evaluate the cytocompatibility of the GMCS. Figure 5 showed that the free MMT is highly cytotoxic. The MMT powders were found aggregating and adhering onto the cell surface. They then destroyed the cell membrane of and penetrated into the cells, resulting in massive loss of cytoplasmic inclusion and cell death.[16] All of the cells
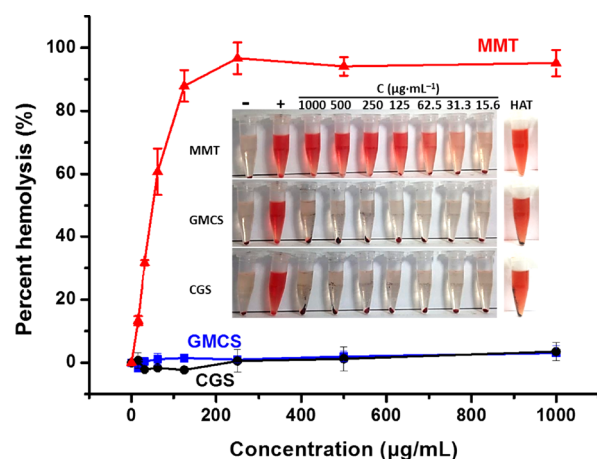
Figure 4. Hemolysis assays for the GMCS, the CGS, and the MMT. Inset: Representative optical photographs show no significant hemoglobin leakage from the GMCS treated RBSs as compared to the positive control. (+) and (−) represent positive and negative control groups, respectively. Hemoglobin absorption tests (HAT) show that the hemoglobin absorption of the corresponding materials is unapparent. Data values corresponded to mean ± SD ($n = 3$).

completely collapsed at the dosage of 250 μg mL^{-1}, leaving lots of cell fragments in the plates (Figure 5A), while at the dosage of 62.5 μg mL^{-1}, most of the cells were oncotic death with blebs (Figure 5B).[16,35] In contrast, the GMCS showed less cytotoxicity (Figure 5C and D). Most of the cells had clear profiles, spread well, and displayed extended and out-stretched morphologies. These evaluations confirmed that the GMCS is also cytocompatible.

3.5. Hemostatic Mechanism. Although MMT in the GMCS cannot directly be in touch with blood, the hemostatic performance of the GMCS has a considerable promotion as compared to that of the CGS.[21] Therefore, with the aim of clarifying the hemostatic mechanism, morphology studies of hemocytes and platelets on the surface of the GMCS were carried out.[22] First, selective adhesion of hemocytes was investigated by incubating the GMCS with the ACD-whole blood in PBS solution (Figure 6A). Figure 6A1 shows that the GMCS does not affect hemocyte's morphology because none of the hemocytes deform or aggregate on the surface of the GMCS. This result is well in agreement with the hemolysis assay. In addition, when the GMCS was incubated with PRP, only a few platelets were found on the GMCS surface (Figure 6A2). Especially, the detected platelets displayed regular resting shape (marked with the white arrows both in Figure 6A2 and in Figure 6A1), suggesting that the GMCS surface did not induce platelets' aggregation or activation in this condition.

Yet, when a droplet of whole blood was dropped onto the GMCS surface (Figure 6B), plasma could be ultrafast absorbed and the entrapped hemocytes aggregated immediately on the material surface, forming a 5 μm thickness of blood-clotting (Figure 6B1). Moreover, when PRP was directly dropped onto the GMCS surface, the platelets stretched out spiny pseudopodia and were trapped with fibrin, forming a cross-linked network (Figure 6B2). This phenomenon has never been found in the previous CGS researches.[21,22] One of the interpretations is that, when the plasma is absorbed into the GMCS, the inside MMT activates Factor XII (also known as Hageman factor in the plasma) to Factor XIIa, a potent activator of prekallikrein that can trigger the intrinsic coagulation pathway and finally form a fibrin network to coagulate blood.[10,11] Therefore, in the synergy of fast absorption of sponge and charge stimulation of MMT, the GMCS achieved an outstanding hemostatic performance.

3.6. Influence of MMT Amount and Scale. Because the additive content of MMT in the GMCS is an influence factor, a series of samples with different MMT contents were prepared. The EDS spectra (Figure 7A) proved the successful preparation of the GMCSs. However, the increased MMT mass attenuates the liquid absorption capability. The GMCS-2 absorbed completely a water/blood droplet within 80 ms, while the GMCS-10 was even a nonabsorbing material, on which a water
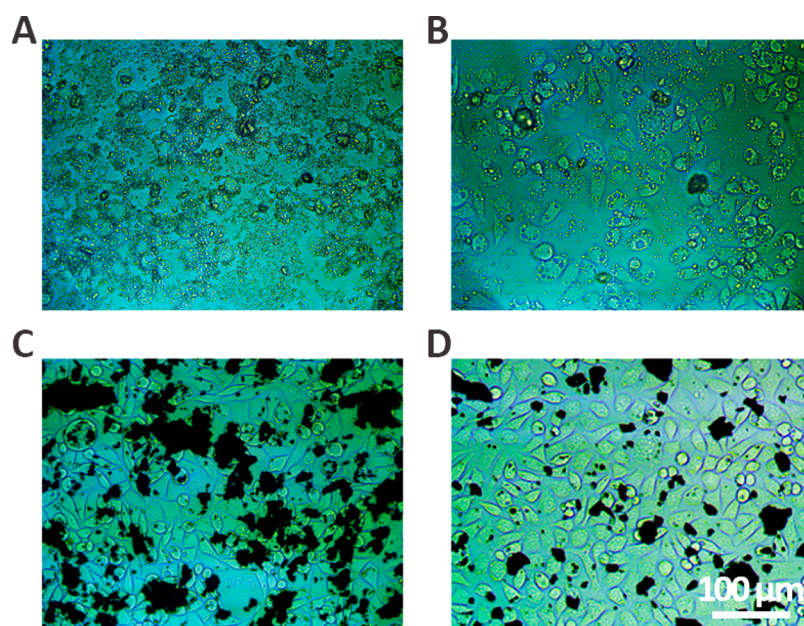

Figure 5. Micrographs of the L929 cells culture under MMT treatments (A,B) and GMCS treatments (C,D), with a dosage of 250 μg mL^{-1} (A,C) and 62.5 μg mL^{-1} (B,D).
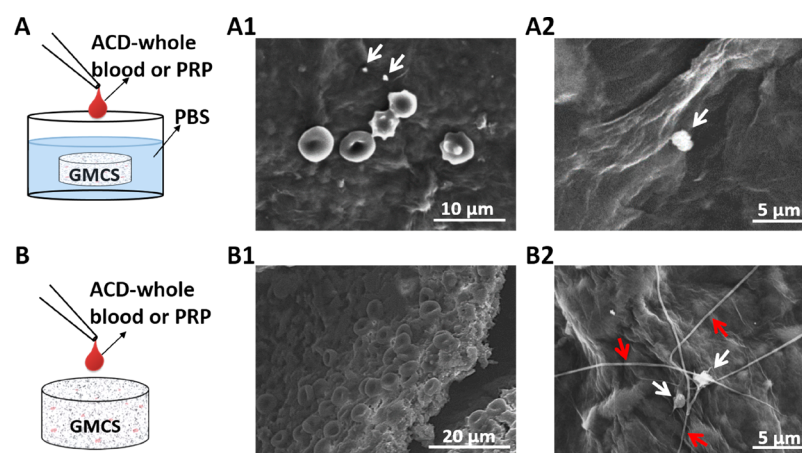
Figure 6. SEM images of interfacial interaction between blood cells and the GMCS, on the basis of two kinds of evaluation model schematically illustrated with (A) and (B), respectively. For pattern A, a droplet of ACD-whole blood or PRP was added into PBS solutions; thus the blood cells (A1) or platelets (A2) could selectively adhere on the surface of the GMCS. For pattern B, a droplet of ACD-whole blood or PRP was directly dropped onto the GMCS; thus the blood cells (B1) or platelets (B2) were forced to adhere to it. The white arrows represent to the platelets, while the red arrows represent to the fibrin.
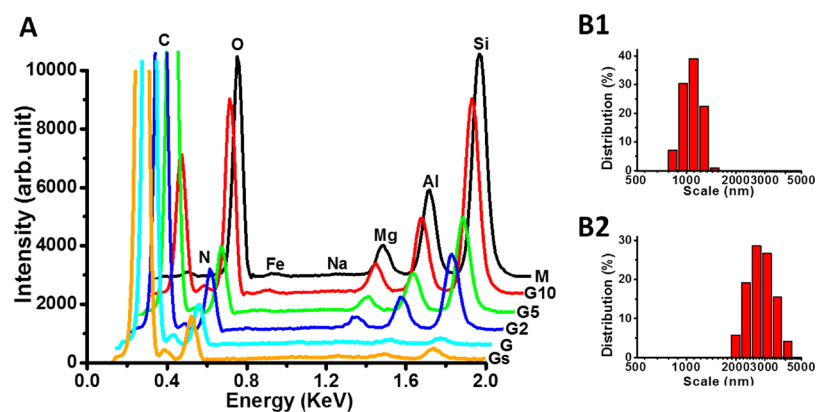

Figure 7. (A) EDS analysis of the GMCSs. The intensity of Si, Al, Mg, and O elements increased with the increase of the MMT mass in the GMCSs. Gs, G, G2, G5, G10, and M represent GMsCS, GMCS, GMCS-2, GMCS-5, GMCS-10, and MMT, respectively. Particle size distribution of (B1) the grinding and (B2) the original MMT.

droplet could stably stand over 14 s. Furthermore, the water (blood) absorption amount of the GMCS-2 decreased to 849.3 ± 70.3 mg cm^{-3} (648.7 ± 82.6 mg cm^{-3}), as compared to the aforementioned 964.4 ± 35.8 mg cm^{-3} (719.5 ± 35.4 mg cm^{-3}) of the GMCS. It was mainly due to the fact that the excess MMT occupied more space in the GMCSs, resulting in less room in the composite for water or blood loading.[36] On the other hand, even though the zeta potential of the GMCS-2 increased to −33.1 ± 1.9 mV (−29.8 ± 1.5 mV for the GMCS), the GMCS-2 showed no enhancement for blood clotting. It stopped bleed at 122 ± 21 s (one-way ANOVA with Tukey's posthoc analysis; $P < 0.05$), which was 37 s longer than that of the GMCS. These data demonstrated that adding more MMT in the GMCSs did not confer faster blood clotting because of the attenuated absorption capacity. Therefore, keeping the liquid absorption capacity of the GMCSs is crucial. It should be the fundamental essence for fast hemostasis of the GMCSs.

An advanced way to enhance charge stimulation without sacrificing blood absorbency is adopting smaller MMT powders. To verify this idea, we kept the MMT mass the same as that in the GMCS, but reduced the particle size of MMT to an average 1.7 ± 0.1 μm (Figure 7B1) from the original 2.8 ± 0.3 μm ($n = 3$, Figure 7B2). The obtained sponge

(denoted as GMsCS) really exhibited water/blood absorbability as fast as 40 ms. The most exciting result was that the GMsCS displayed a shorter hemostatic time. By only using 56 ± 8 s ($n = 3$; one-way ANOVA with Tukey's posthoc analysis; $P < 0.01$), the bleeding was stopped by using the same animal test model.

4. DISCUSSION

The GMCS was demonstrated to be a safe and effective hemostatic. In our viewpoint, it is mainly due to two reasons. One is the novel composite construction. Figure 8 represents the superexcellent match between the cross-linked graphene and MMT sheets in the composite construction. MMT is a typically layered silicate structure. Each layer is composed of two tetrahedral silica sheets sandwiching an octahedral sheet formed from a metal cation such as Al^{3+} or Mg^{2+}.[19] This structure gives MMT special charge distribution characteristics. Its surface possesses negative charges, while the crystal edge is localized positive charges due to that the broken bonds are unsatisfied valences (Figure 8A).[19] GO is known as a nanosheet due to abundant hydroxyl groups and epoxy groups on its surface, and especially carboxyl groups on the edges of the sheet. When MMT is mixed with GO, there are rich
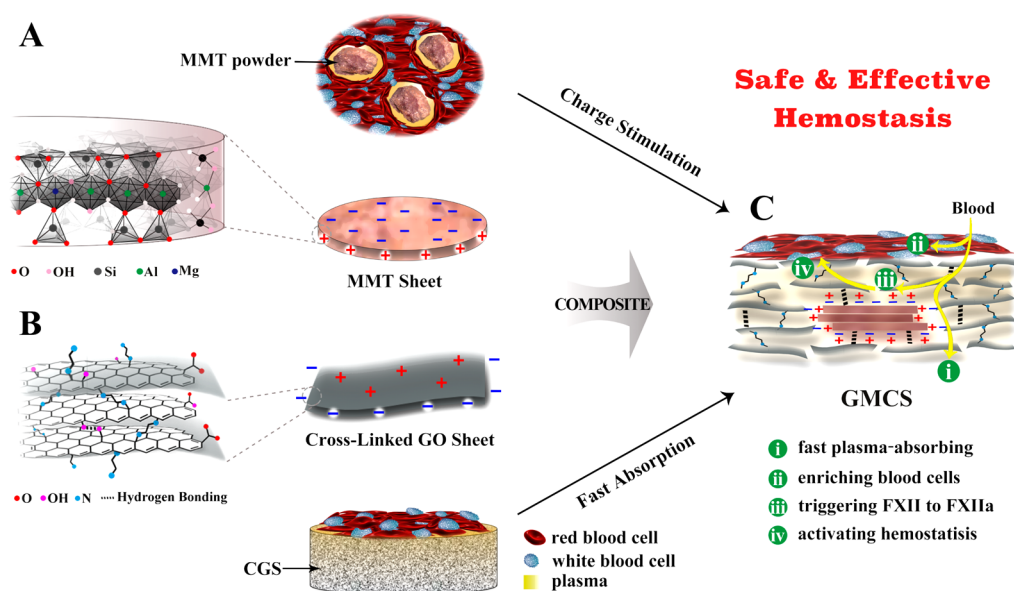
Figure 8. Schematic representation of the GMCS construction and the potential synergy effect for hemostasis. (A) The MMT sheet possesses a permanent negative surface charge and a positive edge arising from the ordered and disordered crystal structures, respectively. Their powders can stimulate in situ clotting of blood with inward hydration and outward activating of blood coagulation. (B) The cross-linked graphene sheet possesses a positive surface charge arising from EDA linkers and a permanent negative edge charge from inherent carboxyl groups. The resulted CGS can absorb plasma rapidly, increasing the concentration of hemocytes and platelets. (C) MMT is fixed in the GMCS by the rich interactions, such as hydrogen bonding and electrostatic interactions. The GMCS changes the blood distribution with (i) fast-absorbing of plasma within the sponge, (ii) concentrating blood on the sponge surface, (iii) activating clotting factors by MMT, and (iv) accelerating the speed of blood clotting, totally resulting in an ultrafast hemostasis.

interactions between them, such as hydrogen-bonding and electrostatic interactions. These interactions make micro MMT powders disperse evenly in GO solution and be anchored by GO nanosheets. With help from the cross-linker EDA, the formed graphene sheet possesses positive charges on its surface and still negative charges on its edge (Figure 8B). Thus, the MMT powder is compounded within graphene sheets tightly, preventing its leakage from the GMCS.

This stable composite structure ensures the biosafety of the GMCS. Previous studies revealed that the free MMT could destruct hemocytes, resulting in cytotoxicity and even thrombosis.[14,15] While preventing direct interaction between MMT with cells, the MMT-containing materials could be safe in biomedical usage. No significant change was seen in the viability of the related cells.[16] For the GMCS, MMT was embedded in the cross-linked graphene sheets and could not be directly in touch with cells. Thus, the cytotoxicity of MMT can be sharply reduced. Besides, graphene to a certain degree is biocompatible and has been widely studied in the fields of biomedicine and pharmaceutical.[37−40] Our previous studies also confirmed that the CGS is hemocompatible.[21,22]

In addition, 2D graphene sheets overmatch one-dimensional (1D) linear polymers or fibers in the composite construction because the latter relatively easily results in leakage of composited powders.[15,19,41] Although polymer/MMT porous scaffolds were studied as hemostasis,[15] it was faultiness maybe due to that the polymer is a flexible 1D linear molecule.[19] The combination between polymer and MMT is unstable. Although MMT may contribute advantages for polymer-based composite,[36,42,43] such as reduced swelling and slowed degradation, it still has more opportunities to leak from the composite, resulting in biotoxicity. In contrast, graphene is a 2D sheet, and it can cover the MMT powder completely. This stiff embedding ensures the substantial binding of MMT. Thus, the biotoxicity of MMT is largely reduced, and the GMCS can be used as a safe hemostasis.

Therefore, we consider that the GMCS achieves rapid hemostasis through fast absorbability and charge stimulation. Essentially, changing the blood distribution is the main reason (Figure 8C). First, the GMCS fast absorbs plasma and enriches blood cells on its surface. Next, the absorbed plasma enters into the inside of the GMCS and contacts with MMT. The rich electrochemistry of MMT facilitates a wide range of possible interactions and affinities with proteins that are in the plasma.[44,45] Especially, Factor XII, which is a serine protease zymogen, combines with the negative charged surface of MMT. Third, Factor XII is induced to change conformation and forms a surface-bound Factor XIIa, which contains two polypeptide chains linked by a disulfide bond.[10,11] Finally, the disulfide bond is cleavage, and Factor XIIa is free to diffuse into the plasma, which triggers the intrinsic pathway of blood coagulation.[10,11] In this hemostatic process, the first step of the fast plasma absorption is crucial for the GMCS. The enriched blood cells by the GMCS will induce and accelerate blood clotting.[21,22] Yet when MMT is used as hemostatic alone (Figure 8A), regardless of the side effects, the naked MMT will enrich blood cells through absorbing plasma and swelling upon hydration. This process is relatively localized and slow,[46,47] and the enriched blood cells that are on the surface of MMT may form a barrier to block the outside Factor XII to contact with the inner MMT, thus reducing hemostatic efficiency. Moreover, as compared to the limited tank of the MMT powder, the GMCS can be considered as an infinite space. More plasma can be absorbed efficiently inside of the GMCS, thus not only increasing the interactions between MMT and Factor XII, but also enhancing the release of the generated Factor XIIa and its stimulation. In any case, this composite of the cross-linked graphene and MMT maximizes their contribution to hemostasis.

Nowadays, hemostatic agents with different hemostatic mechanisms are widely developed. For example, the common used zeolite and mesoporous silica stop bleeding by quick plasma absorbability to increase the concentration of blood cells. Besides, chitosan-based hemostatic materials promote blood clotting through charge stimulation of the clotting factors. However, it should be cautioned that using large amounts of minerals or natural polymers may cause associated complications or allergies.[48] As compared to these traditional hemostatics, the GMCS contains less organic EDA linkers (less than 3% w/w) and inorganic MMT powders (less than 10^{-6} v/ v) that ensures the biosafety of the GMCS. By adding a small amount of MMT, the GMCS can rapidly stop bleeding in the synergy of fast absorption of sponge and charge stimulation of MMT. Therefore, the GMCS is a safe and effective hemostatic material.

5. CONCLUSIONS

In summary, we developed a novel trauma hemostatic material, the GMCS, which can rapidly stop bleeding in 85 s in rabbit artery injury test. The GMCS promotes blood coagulation not only by quickly absorbing plasma to increase the concentration of hemocytes and platelets on the wound surface, but also by activating Hageman factor (Factor XII) with MMT's surface charges to trigger the intrinsic pathway of blood coagulation. Although the addition amount of MMT is too small to compare to the way of using MMT powders directly, its hemostatic action is fully played out within the GMCS. A synergy effect is remarkably showed in this composite, where the dimension changes of blood distribution play a crucial role. In-depth insight demonstrated that adding a suitable amount and size of MMT powders (no more than 1 mg mL^{-1} with the diameter less than 2 μm) in the GMCS is in favor of enhancing the hemostatic performance, while it does not scarify the GMCS's absorbability. More importantly, the GMCS did not cause in vivo thrombus or blood clot in the vessels. Biocompatibility evaluations further highlighted the cytocompatibility of this GMCS material. Significantly, this GMCS hemostatic employed less organic ingredient (less than 3% w/w EDA linkers) and inorganic powders (less than 10^{-6} v/v). As compared to traditional hemostatics, the GMCS has many advantages, such as facile preparation, low cost, portability, long shelf life, and nontoxicity. Therefore, we anticipated that this study could not only provide a new strategy for MMT used in the hemostatic field again, but also open a new avenue to develop a superb GMCS-type hemostat used for trauma therapy. Because many kinds of clay powders, such as bentonite, diatomite, and halloysite, are the isostructures of MMT, all of them can be used as infillings to add into the graphene-based sponge. Furthermore, this graphene-stimuli composite sponge can act as a platform to introduce different hemostatic mechanisms, providing broad space for future development of novel hemostatic materials.

■ AUTHOR INFORMATION

Corresponding Author

*Tel.: +861064447747. Fax: +861064416428. E-mail: wangxing@mail.buct.edu.cn.

ORCID Ⓞ

Xing Wang: 0000-0002-9990-1479

Notes

The authors declare no competing financial interest.

■ REFERENCES

(1) Sauaia, A.; Moore, F. A.; Moore, E. E.; Haenel, J. B.; Read, R. A.; Lezotte, D. C. Early Predictors of Postinjury Multiple Organ Failure. *Arch. Surg.* 1994, 129, 39−45.

(2) Cosgriff, N.; Moore, E. E.; Sauaia, A.; Kenny-Moynihan, M.; Burch, J. M.; Galloway, B. Predicting Life-Threatening Coagulopathy in the Massively Transfused Trauma Patient: Hypothermia and Acidoses Revisited. *J. Trauma* 1997, 42, 857−862.

(3) Heckbert, S. R.; Vedder, N. B.; Hoffman, W.; Winn, R. K.; Hudson, L. D.; Jurkovich, G. J.; Copass, M. K.; Harlan, J. M.; Rice, C. L.; Maier, R. V. Outcome after Hemorrhagic Shock in Trauma Patients. *J. Trauma* 1998, 45, 545−549.

(4) Sauaia, A.; Moore, F. A.; Moore, E. E.; Moser, K. S.; Brennan, R.; Read, R. A.; Pons, P. T. Epidemiology of Trauma Deaths: a Reassessment. *J. Trauma* 1995, 38, 185−193.

(5) Chan, L. W.; Wang, X.; Wei, H.; Pozzo, L. D.; White, N. J.; Pun, S. H. A Synthetic Fibrin Cross-Linking Polymer for Modulating Clot Properties and Inducing Hemostasis. *Sci. Transl. Med.* 2015, 7, 277ra29−277ra29.

(6) Chimene, D.; Alge, D. L.; Gaharwar, A. K. Two-Dimensional Nanomaterials for Biomedical Applications: Emerging Trends and Future Prospects. *Adv. Mater.* 2015, 27, 7261−7284.

(7) Howe, N.; Cherpelis, B. Obtaining Rapid and Effective Hemostasis: Part I. Update and Review of Topical Hemostatic Agents. *J. Am. Acad. Dermatol.* 2013, 69, 659.e1−659.e17.

(8) Gaharwar, A. K.; Avery, R. K.; Assmann, A.; Paul, A.; McKinley, G. H.; Khademhosseini, A.; Olsen, B. D. Shear-Thinning Nano-composite Hydrogels for the Treatment of Hemorrhage. *ACS Nano* 2014, 8, 9833−9842.

(9) Manias, E.; Touny, A.; Wu, L.; Strawhecker, K.; Lu, B.; Chung, T. Polypropylene/Montmorillonite Nanocomposites. Review of the Synthetic Routes and Materials Properties. *Chem. Mater.* 2001, 13, 3516−3523.

(10) Baker, S. E.; Sawvel, A. M.; Zheng, N.; Stucky, G. D. Controlling Bioprocesses with Inorganic Surfaces: Layered Clay Hemostatic Agents. *Chem. Mater.* 2007, 19, 4390−4392.

(11) Griffin, J. H. Role of Surface in Surface-Dependent Activation of Hageman Factor (Blood Coagulation Factor XII). *Proc. Natl. Acad. Sci. U. S. A.* 1978, 75, 1998−2002.

(12) Kheirabadi, B. S.; Edens, J. W.; Terrazas, I. B.; Estep, J. S.; Klemcke, H. G.; Dubick, M. A.; Holcomb, J. B. Comparison of New Hemostatic Granules/Powders with Currently Deployed Hemostatic Products in a Lethal Model of Extremity Arterial Hemorrhage in Swine. *J. Trauma* 2009, 66, 316−328.

(13) Kheirabadi, B. S.; Scherer, M. R.; Estep, J. S.; Dubick, M. A.; Holcomb, J. B. Determination of Efficacy of New Hemostatic Dressings in a Model of Extremity Arterial Hemorrhage in Swine. *J. Trauma* 2009, 67, 450−460.

(14) Kheirabadi, B. S.; Mace, J. E.; Terrazas, I. B.; Fedyk, C. G.; Estep, J. S.; Dubick, M. A.; Blackbourne, L. H. Safety Evaluation of New Hemostatic Agents, Smectite Granules, and Kaolin-Coated Gauze in a Vascular Injury Wound Model in Swine. *J. Trauma* 2010, 68, 269−278.

(15) Carraway, J. W.; Kent, D.; Young, K.; Cole, A.; Friedman, R.; Ward, K. R. Comparison of a New Mineral Based Hemostatic Agent to a Commercially Available Granular Zeolite Agent for Hemostasis in a Swine Model of Lethal Extremity Arterial Hemorrhage. *Resuscitation* 2008, 78, 230−235.

(16) Bowman, P. D.; Wang, X.; Meledeo, M. A.; Dubick, M. A.; Kheirabadi, B. S. Toxicity of Aluminum Silicates Used in Hemostatic Dressings Toward Human Umbilical Veins Endothelial Cells, HeLa

Cells, and RAW267. 4 Mouse Macrophages. *J. Trauma* **2011**, *71*, 727−732.

(17) Ul-Islam, M.; Khan, T.; Khattak, W. A.; Park, J. K. Bacterial Cellulose-MMTs Nanoreinforced Composite Films: Novel Wound Dressing Material with Antibacterial Properties. *Cellulose* **2013**, *20*, 589−596.

(18) Sandri, G.; Bonferoni, M. C.; Ferrari, F.; Rossi, S.; Aguzzi, C.; Mori, M.; Grisoli, P.; Cerezo, P.; Tenci, M.; Viseras, C. Montmorillonite−Chitosan−Silver Sulfadiazine Nanocomposites for Topical Treatment of Chronic Skin Lesions: in vitro Biocompatibility, Antibacterial Efficacy and Gap Closure Cell Motility Properties. *Carbohydr. Polym.* **2014**, *102*, 970−977.

(19) Dawson, J. I.; Oreffo, R. O. Clay: New Opportunities for Tissue Regeneration and Biomaterial Design. *Adv. Mater.* **2013**, *25*, 4069−4086.

(20) Vaiana, C. A.; Leonard, M. K.; Drummy, L. F.; Singh, K. M.; Bubulya, A.; Vaia, R. A.; Naik, R. R.; Kadakia, M. P. Epidermal Growth Factor: Layered Silicate Nanocomposites for Tissue Regeneration. *Biomacromolecules* **2011**, *12*, 3139−3146.

(21) Quan, K.; Li, G.; Luan, D.; Yuan, Q.; Tao, L.; Wang, X. Black Hemostatic Sponge Based on Facile Prepared Cross-Linked Graphene. *Colloids Surf., B* **2015**, *132*, 27−33.

(22) Quan, K.; Li, G.; Tao, L.; Xie, Q.; Yuan, Q.; Wang, X. Diaminopropionic Acid Reinforced Graphene Sponge and Its Use for Hemostasis. *ACS Appl. Mater. Interfaces* **2016**, *8*, 7666−7673.

(23) Hummers, W. S., Jr; Offeman, R. E. Preparation of Graphitic Oxide. *J. Am. Chem. Soc.* **1958**, *80*, 1339−1339.

(24) Liao, K.-H.; Lin, Y.-S.; Macosko, C. W.; Haynes, C. L. Cytotoxicity of Graphene Oxide and Graphene in Human Erythrocytes and Skin Fibroblasts. *ACS Appl. Mater. Interfaces* **2011**, *3*, 2607−2615.

(25) Gu, R.; Sun, W.; Zhou, H.; Wu, Z.; Meng, Z.; Zhu, X.; Tang, Q.; Dong, J.; Dou, G. The Performance of a Fly-Larva Shell-Derived Chitosan Sponge as an Absorbable Surgical Hemostatic Agent. *Biomaterials* **2010**, *31*, 1270−1277.

(26) Maiti, M.; Bhowmick, A. K. New Fluoroelastomer Nanocomposites from Synthetic mMontmorillonite. *Compos. Sci. Technol.* **2008**, *68*, 1−9.

(27) Seyama, H.; Soma, M. X-Ray Photoelectron Spectroscopic Study of Montmorillonite Containing Exchangeable Divalent Cations. *J. Chem. Soc., Faraday Trans. 1* **1984**, *80*, 237−248.

(28) Kevadiya, B. D.; Chettiar, S. S.; Rajkumar, S.; Bajaj, H. C.; Brahmbhatt, H.; Chaudhari, J. C.; Thumbar, R. P.; Jhala, D.; Rao, M. V. Evaluation of Montmorillonite/Poly (L-Lactide) Microcomposite Spheres as Ambidextrous Reservoirs for Controlled Release of Capecitabine (Xeloda) and Assessment of Cell Cytotoxic and Oxidative Stress Markers. *Compos. Sci. Technol.* **2014**, *90*, 193−201.

(29) Bu, Y.; Zhang, L.; Liu, J.; Zhang, L.; Li, T.; Shen, H.; Wang, X.; Yang, F.; Tang, P.; Wu, D. Synthesis and Properties of Hemostatic and Bacteria-Responsive in Situ Hydrogels for Emergency Treatment in Critical Situations. *ACS Appl. Mater. Interfaces* **2016**, *8*, 12674−12683.

(30) Chen, F.; Cao, X.; Chen, X.; Wei, J.; Liu, C. Calcium-Modified Microporous Starch with Potent Hemostatic Efficiency and Excellent Degradability for Hemorrhage Control. *J. Mater. Chem. B* **2015**, *3*, 4017−4026.

(31) Berger, J.; Reist, M.; Mayer, J. M.; Felt, O.; Peppas, N. A.; Gurny, R. Structure and Interactions in Covalently and Ionically Crosslinked Chitosan Hydrogels for Biomedical Applications. *Eur. J. Pharm. Biopharm.* **2004**, *57*, 19−34.

(32) Sasidharan, A.; Panchakarla, L. S.; Sadanandan, A. R.; Ashokan, A.; Chandran, P.; Girish, C. M.; Menon, D.; Nair, S. V.; Rao, C.; Koyakutty, M. Hemocompatibility and Macrophage Response of Pristine and Functionalized Graphene. *Small* **2012**, *8*, 1251−1263.

(33) Singh, S. K.; Singh, M. K.; Nayak, M. K.; Kumari, S.; Shrivastava, S.; Grácio, J. J.; Dash, D. Thrombus Inducing Property of Atomically Thin Graphene Oxide Sheets. *ACS Nano* **2011**, *5*, 4987−4996.

(34) Singh, S. K.; Singh, M. K.; Kulkarni, P. P.; Sonkar, V. K.; Grácio, J. J.; Dash, D. Amine-Modified Graphene: Thrombo-Protective Safer Alternative to Graphene Oxide for Biomedical Applications. *ACS Nano* **2012**, *6*, 2731−2740.

(35) Majno, G.; Joris, I. Apoptosis, Oncosis, and Necrosis. An Overview of Cell Death. *Am. J. Pathol.* **1995**, *146*, 3−3.

(36) Ul-Islam, M.; Khan, T.; Park, J. K. Nanoreinforced Bacterial Cellulose-Montmorillonite Composites for Biomedical Applications. *Carbohydr. Polym.* **2012**, *89*, 1189−1197.

(37) Sun, Y.; Wang, S.; Li, C.; Luo, P.; Tao, L.; Wei, Y.; Shi, G. Large Scale Preparation of Graphene Quantum Dots from Graphite with Tunable Fluorescence Properties. *Phys. Chem. Chem. Phys.* **2013**, *15*, 9907−9913.

(38) Dong, H.; Dai, W.; Ju, H.; Lu, H.; Wang, S.; Xu, L.; Zhou, S.-F.; Zhang, Y.; Zhang, X. Multifunctional Poly (L-Lactide)-Polyethylene Glycol-Grafted Graphene Quantum Dots for Intracellular MicroRNA Imaging and Combined Specific-Gene-Targeting Agents Delivery for Improved Therapeutics. *ACS Appl. Mater. Interfaces* **2015**, *7*, 11015−11023.

(39) Rodrigo, D.; Limaj, O.; Janner, D.; Etezadi, D.; de Abajo, F. J. G.; Pruneri, V.; Altug, H. Mid-Infrared Plasmonic Biosensing with Graphene. *Science* **2015**, *349*, 165−168.

(40) Yang, K.; Wan, J.; Zhang, S.; Tian, B.; Zhang, Y.; Liu, Z. The Influence of Surface Chemistry and Size of Nanoscale Graphene Oxide on Photothermal Therapy of Cancer Using Ultra-Low Laser Power. *Biomaterials* **2012**, *33*, 2206−2214.

(41) Yang, S.; Feng, X.; Ivanovici, S.; Müllen, K. Fabrication of Graphene-Encapsulated Oxide Nanoparticles: Towards High-Performance Anode Materials for Lithium Storage. *Angew. Chem.* **2010**, *122*, 8586−8589.

(42) Corrales, T.; Larraza, I.; Catalina, F.; Portolés, T.; Ramírez-Santillán, C.; Matesanz, M.; Abrusci, C. In vitro Biocompatibility and Antimicrobial Activity of Poly (ε-Caprolactone)/Montmorillonite Nanocomposites. *Biomacromolecules* **2012**, *13*, 4247−4256.

(43) Jorge, M. F. C.; Flaker, C. H. C.; Nassar, S. F.; Moraes, I. C. F.; Bittante, A. M. Q. B.; do Amaral Sobral, P. J. Viscoelastic and Rheological Properties of Nanocomposite-Forming Solutions Based on Gelatin and Montmorillonite. *J. Food Eng.* **2014**, *120*, 81−87.

(44) Talibudeen, O. Complex Formation between Montmorillonoid Clays and Amino-Acids and Proteins. *Trans. Faraday Soc.* **1955**, *51*, 582−590.

(45) Barrientos-Velázquez, A. L.; Arteaga, S.; Dixon, J. B.; Deng, Y. The Effects of pH, Pepsin, Exchange Cation, and Vitamins on Aflatoxin Adsorption on Smectite in Simulated Gastric Fluids. *Appl. Clay Sci.* **2016**, *120*, 17−23.

(46) Luckham, P. F.; Rossi, S. The Colloidal and Rheological Properties of Bentonite Suspensions. *Adv. Colloid Interface Sci.* **1999**, *82*, 43−92.

(47) Norrish, K. The Swelling of Montmorillonite. *Discuss. Faraday Soc.* **1954**, *18*, 120−134.

(48) Achneck, H. E.; Sileshi, B.; Jamiolkowski, R. M.; Albala, D. M.; Shapiro, M. L.; Lawson, J. H. A Comprehensive Review of Topical Hemostatic Agents: Efficacy and Recommendations for Use. *Ann. Surg.* **2010**, *251*, 217−228.